Impact of compositional nonuniformity in (In,Ga)N-based light emitting diodes

A. Di Vito, A. Di Carlo, and M. Auf der Maur*
Department of Electronics Engineering, University of Rome Tor Vergata, Via del Politecnico 1, 00133 Rome, Italy

A. Pecchia
CNR-ISMN, Via Salaria Km 29.300, 00017 Monterotondo (Rome), Italy

Carrier localization due to statistical fluctuations in Indium Gallium Nitride alloys has been recognized to play an important role for light emitting diode performance, both experimentally and through theoretical studies. While usually a random alloy assumption is made, in this work we take into account the presence of spatial nonuniformities in the indium content on the nanometer scale, and we theoretically analyze its impact on the electronic and optical properties of the alloy and the device. We show that indium clustering induces tail states in both the conduction and valence bands. This causes a reduction of the band gap and a broadening of the optical absorption edge. Furthermore, compositional fluctuations in the active region of the device determine a substantial broadening of the optical emission spectrum and a decrease of the peak emission energy, in agreement with experimental results. Moreover, the radiative recombination coefficient increases for increasing degree of clustering, suggesting a transition to a quantum dot like structure. Finally, the temperature dependence of the radiative coefficient derived for the nonuniform structures is in good agreement with the experimental results, that show a temperature behavior opposite to the trend expected from standard theoretical considerations.

I. INTRODUCTION

Indium Gallium Nitride is a successful material for the realization of efficient short-wavelength commercial light emitting diodes (LEDs) [1–3]. As a matter of fact, InGaN potentially covers the whole visible spectrum, thus allowing in principle to eliminate the phosphor based down conversion and enabling a color mixing approach, which would allow to further increase overall white LED efficiency [4].

Although the technology for InGaN based blue and white LEDs has been successfully commercialized, there are several material related issues, such as efficiency droop, green gap, compositional nonuniformity and spatial localization of carriers, which are still under debate [5–11]. While structural characterisation reveals a compositional uniformity compatible with the assumption of a random alloy in high quality structures [12], one should expect some deviation from such an idealized structure on the atomic scale. Previous studies show that the fluctuations in the local indium concentration, even in the case of a uniform random alloy, lead to translational symmetry breaking and carrier spatial localization [13–18]. Interestingly, the hole localization, particularly evident in samples containing indium clusters, appears to have a strong influence on the alloy properties [19, 20].

In most of the studies conducted so far, the impact of deviations from a uniform random alloy on the properties of InGaN has not been discussed [7, 8, 13, 14, 21, 22]. Furthermore, the theoretical analysis based on density functional theory (DFT) performed on clustered InGaN bulk structures [23, 24] lack a properly large supercell size and a sufficiently large number of random samples. Thus, a discussion of the role of clustering for the properties of InGaN alloys and the performances of InGaN based LEDs, supported by a proper statistical characterization of the samples, is still needed.

In the present work, we theoretically describe the optical properties of bulk InGaN alloys and InGaN/GaN single quantum well (SQW) LEDs, taking into account the statistical fluctuation of the alloy composition and the presence of indium clusters. In particular, we study the transition from a perfect random alloy towards a nonuniform one. In Sec. II we present the theoretical approach used to perform the simulations and we describe in detail the method employed to generate the samples with several amounts of nonuniformity. The results of the simulations are shown in Sec. III A and Sec. III B for the bulk material and the device, respectively. We analyze the outcomes of our study and compare them with the experimental measurements, in terms of energy gap, optical absorption coefficient, emission spectra and temperature dependence of the radiative coefficient. We discuss the influence of compositional nonuniformity on the optical properties of both the bulk alloy and the device.

II. THEORETICAL APPROACH

In order to theoretically study the effect of alloy nonuniformity on macroscopic device performance we use a computational scheme combining continuum and atomistic models. To obtain the electronic and optical properties of both the bulk material and the device, we use an atomistic empirical tight binding (ETB) approach [25, 26]. The atomistic structures are first relaxed using a Keating valence force field (VFF) method [27]. The parameters α and β of the model are computed to re-

* auf.der.maur@ing.uniroma2.it

produce the bulk elasticity tensor of the pure materials. In the random alloy, for each In-N and Ga-N bond, we use the corresponding bulk values for α and β. Then, we compute the electron and hole states from which we calculate the momentum matrix elements, optical spectra and density of states.

For the simulations of the bulk material, we compute the first twelve electron and twenty-four hole states at the Γ point of the Brillouin zone. We use 10 $\times$ 10 $\times$ 10 nm^3 periodic supercells with a mean indium content of $x = 20\%$, corresponding to a value laying in between those needed to obtain blue and green quantum well light emitting diodes. The qualitative results and trends demonstrated in this study, though, are valid for the whole range of technologically relevant indium content values.

The random alloy samples are generated by substituting gallium atoms with indium atoms randomly, assuming a spatially uniform substitution probability equal to the mean indium concentration. Differently, for the nonuniform alloy we first distribute uniformly a certain percentage of indium atoms, which we denote in the following as the percentage of uniformity in order to identify different structures. The remaining indium atoms are then distributed with a spatially varying probability as follows. We first pick randomly a gallium atom. Then we count the indium atoms around this gallium up to the second nearest cation site, and we calculate the substitution probability as the ratio of this number and the available cation sites, leading therefore to a spatial correlation. This is repeated until all necessary indium atoms are distributed. Note that the total number of indium atoms is always the same, in order to fix the mean indium content.

The degree of clustering can be controlled by the percentage of uniformly distributed indium atoms, for which we use values of 100% (random alloy), 80%, 60% and 40% of the total number of indium atoms. The lower the percentage, the more clustering can be expected. To obtain statistically significant results, we simulate 50 structures for the uniform random alloy configuration, as well as for the slightly clustered alloy (80% uniformity). For the other cases we use 100 random samples, since the statistical variations are more pronounced for the strongly clustered samples.

For the InGaN/GaN SQW LED we used a structure as shown schematically in Fig. 1, assuming a mean indium content of $x = 20\%$ and a well width of 3 nm. The considered device has the same structural parameters as those used for the calculations performed by Auf der Maur *et al.* [7]. As a matter of fact, the present work can be retained as an extension of the mentioned study, where the nonuniformity of the InGaN alloy was not addressed. Although spatial variations of the QW thickness can be expected in real LEDs, which influence device behavior as shown e.g. in [22, 28], we assumed here ideal QW inerfaces in order to not mix different effects in our study. However, well width variations could

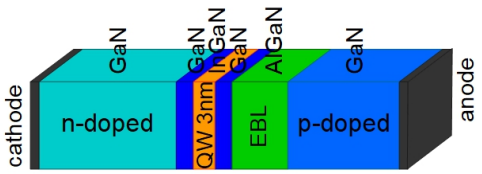

FIG. 1. Schematic view of the simulated structure.

be taken into account in our simulation model, using an approach similar to that in the analysis of Tanner *et al.* [22].

All simulations have been performed for a LED operating point close to the maximum internal quantum efficiency, and a periodic supercell of 10×10 nm^2 is chosen in the quantum well plane. To obtain the electrostatic potential, needed to set up the tight-binding Hamiltonian, and the quasi Fermi levels at the chosen operating point, we first solve the 1D Schrödinger/drift-diffusion problem, using TiberCAD software [29]. The potential is then projected onto the atomic positions, neglecting thus variations in the QW plane. For the calculation of the optical spectra, we compute the first eight electron and twelve hole states in the Γ, M, X and Y points of the reduced Brillouin zone, and we use the trapezoidal method for reciprocal space integration.

III. RESULTS AND DISCUSSION

In this section, we show the results of the simulations performed for the $In_{0.2}Ga_{0.8}N$ alloy (Sec. III A) and the InGaN/GaN SQW LED (Sec. III B), where the fluctuations of the indium content are taken into account. We analyze the outcomes of our theoretical derivation and discuss the comparison with the experimental measurements. We demonstrate that it is crucial to consider the presence of compositional nonuniformity in order to properly describe the optical properties of both the bulk material and the device.

A. Bulk $In_{0.2}Ga_{0.8}N$ Alloy

In Fig. 2 we show the mean density of states (DOS), i.e. the weighted sum of the DOS of all random samples. We can clearly see that indium clustering yields tail states both in the conduction and valence bands and reduces the band gap by approximately 0.5 eV compared to the uniform alloy, confirming the results reported in previous studies [24, 30–32]. Moreover, the band gap values calculated taking into account the nonuniformities of the samples are in reasonable agreement with the experimental data found in literature[33–35], as reported in Table I for completeness. Note that for the random alloy case only an insignificant broadening of the band edges is

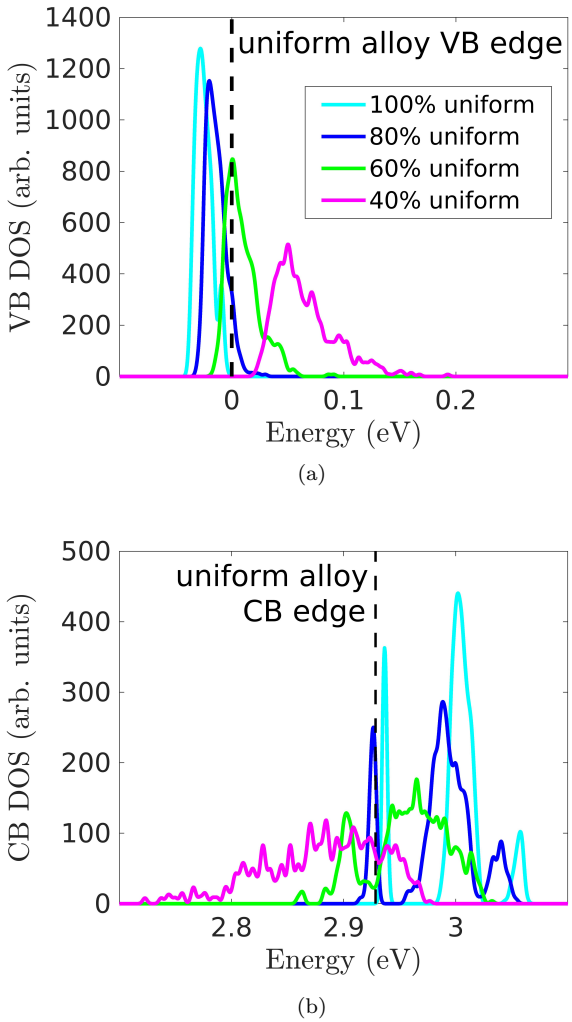

FIG. 2. Density of states (sample average) for a bulk $In_{0.2}Ga_{0.8}N$ alloy with several percentage of uniformly distributed indium atoms, resulting in several degrees of clustering. The valence and conduction band states are represented in a) and b), respectively.

predicted. These band tails are due to the strong scattering in the energies of the electron and hole ground states, which increases with increasing deviation from a uniform alloy. This effect is associated with increasing localization of the carrier wave functions, which is correlated with the degree of indium clustering [36].

Concerning the optical properties of the clustered bulk $In_{0.2}Ga_{0.8}N$ alloy, it is particularly interesting to analyze the behavior of the absorption spectrum, shown in Fig. 3. We observe an increasing broadening of the optical absorption edge with increasing clustering degree, and washing out of a double peak structure at the absorption edge. This trends are in good agreement with the experimental results reported by Butté *et al.* [37] on thick InGaN layers, at least under the reasonable assumption that growing indium content leads to increased nonuniformity. Thus, the optical absorption edge broadening

TABLE I. Calculated and measured energy gap values. The theoretical results are reported for the uniform alloy and the structure with the highest clustering degree. The experimental values #1, #2 and #3 refer to the studies of Wu *et al.* [33] (absorption measurements), Moret *et al.* [35] and Franssen *et al.* [34] (PL measurements), respectively.

	Energy Gap [eV]
this work	2.9 $\xrightarrow{\text{clustering}}$ 2.5
Exp#1	2.7
Exp#2	2.5
Exp#3	2.4

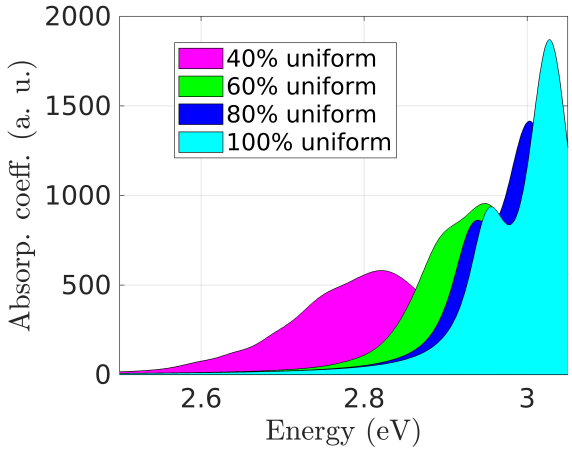

FIG. 3. Absorption coefficient (sample average) for a bulk $In_{0.2}Ga_{0.8}N$ alloy with several percentage of uniformly distributed indium atoms, resulting in several degrees of clustering.

observed by Butté *et al.* could be explained by increasing nonuniformity in the indium distribution.

B. InGaN/GaN SQW-LED

The mean emission spectra of the InGaN/GaN SQW LED are shown in Fig. 4 for each considered percentage of uniformly distributed indium atoms. The band gap reduction, induced by the nonuniformity of the alloy composition, yields a red-shift of the peak emission energy as the indium clustering degree increases. Moreover, it can be seen that indium clustering induces a pronounced broadening of the spectrum. The measured emission spectrum of a SQW LED with a structure similar to the simulated one but slightly lower indium content [38] is represented by the gray area in Fig. 4. Note that both the measured peak position and spectrum width are better described by the model with a nonuniform alloy. In particular, the case of 60% uniformity seems to reproduce rather well the experimental features. The high energy tail is well described, while the low energy tail shows slightly too little broadening. Note that the

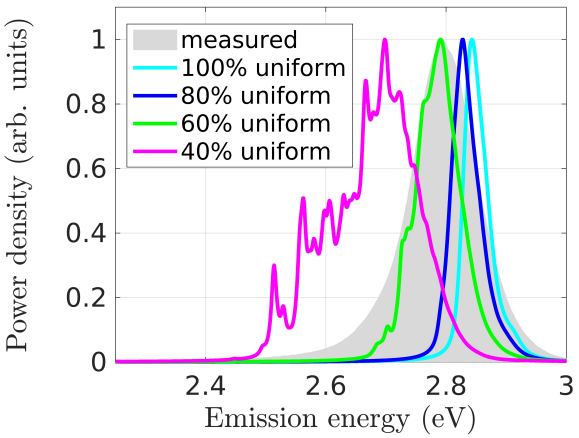

FIG. 4. Calculated emission spectra (sample average) for an $In_{0.2}Ga_{0.8}N$ quantum well at several percentage of uniformity. The experimental spectrum [38] is depicted by the gray area.

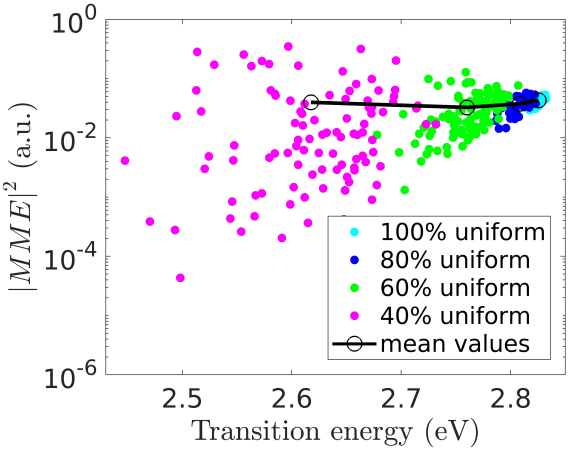

FIG. 5. Ground state transition MME, i.e. the MME related to the optical transition from the electron ground state to the hole ground state, of an $In_{0.2}Ga_{0.8}N$ quantum well calculated at Γ point for several percentage of uniformity. The results for each simulated sample are visualized as dots while the sample average is labeled by black circles.

60% uniform samples are consistent with the atom probe tomography (APT) measurements reported in literature [9, 28] if the limited APT detection efficiency is taken into account [39]. This is discussed in detail in Sec. I of the Supplemental Material [36], where we analyze the indium distribution within the $In_{0.2}Ga_{0.8}N$ supercell for all the considered percentage of uniformity.

A scatter plot of the ground state momentum matrix elements (MME) evaluated at the Γ point of the Brillouin zone for all the simulated structures and for each percentage of uniformity is shown in Fig. 5. It can be seen that the increase of clustering degree causes an increasing spread in the calculated MME values. This behavior is due to the fact that the carriers' localization induced by compositional fluctuations yields substantial statistical variations in the electron and hole wave functions overlap. This is illustrated in Fig. 6, where the ground state electron and hole wave functions for the structures with minimum and maximum MME are shown for the largest degree of clustering studied (40% of uniformity). Furthermore, we can see in Fig. 5 that the MME average value slightly decreases for small nonuniformity (up to 60% of uniformity) and then increases for the 40% uniform case. This is because, with substantial alloy nonuniformity, the indium clustering may localize both electrons and holes in the same spatial position, overcoming the quantum confined Stark effect (QCSE), as is the case in the left panel of Fig. 6. Indeed, in such a case the MME can be considerably larger than that of the random alloy. Otherwise, due to QCSE, the electron and hole states are influenced by the largely independent indium content fluctuations near the upper and lower QW interface, respectively[7].

The radiative recombination coefficient B for all the simulated structures and each considered percentage of uniformity is shown in Fig. 7. The B value for each structure is calculated assuming constant quasi Fermi levels

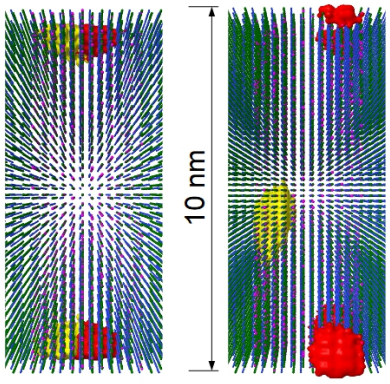

FIG. 6. Ground state electron (red) and hole (yellow) wave functions for the $In_{0.2}Ga_{0.8}N$ quantum well with 40% (maximum clustering degree) of uniformly distributed indium atoms. Two structures are represented, corresponding to (right) the minimum and (left) the maximum value of MME. The isosurfaces containing 50% of the total ground state density are shown. Indium, gallium and nitrogen atoms are depicted in magenta, green and blue, respectively.

such that the mean carrier density is fixed and equal to $\bar{n} = \bar{p} = 5 \times 10^{11}$ cm^{-2}. The global radiative coefficient is defined as $\bar{B} = \bar{R}_r/(\bar{n}\bar{p})$, where $\bar{R}_r$ is the mean radiative recombination rate, i.e. the weighted sum of the radiative recombination rate of all random samples[7]. As expected from the behavior of the MME, the indium clustering induces an increment of the spread in the calculated values of B. However, while the mean ground state transition MME decreases up to 60% of uniformity, the global value of the radiative coefficient increases for increasing nonuniformity. As a matter of fact, a higher number of optical transitions is allowed due to the trans-

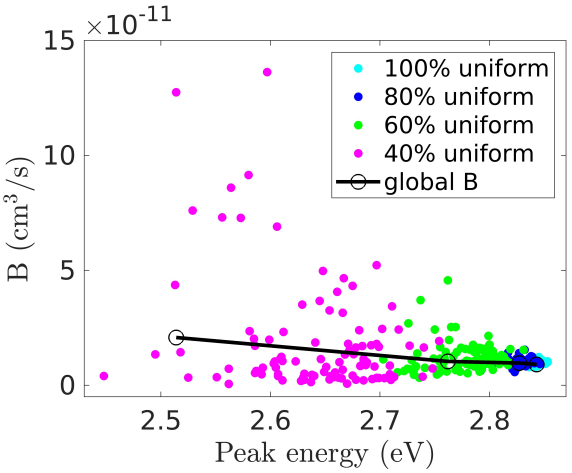

FIG. 7. Radiative recombination coefficient B of an $In_{0.2}Ga_{0.8}N$ quantum well for several percentage of uniformity. The results for each simulated sample are visualized as dots and the global B is labeled by black circles.

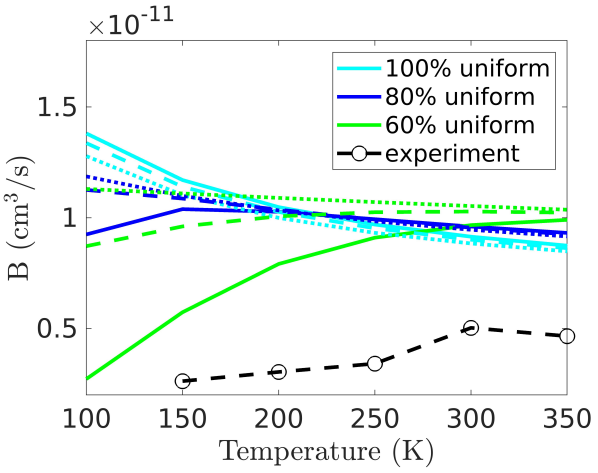

FIG. 8. Temperature dependence of B for an $In_{0.2}Ga_{0.8}N$ quantum well at several percentage of uniformly distributed indium atoms. The solid, dashed and dotted lines represent the values obtained for a mean carrier density of 10^{11}, 5×10^{11} and 10^{12} cm^{-2}, respectively. The experimental behavior [19] derived for a mean carrier density of approximately 10^{12} cm^{-2} [41] is labeled by black circles. The results for the 40% uniform structure are not reported in the figure, since their range of variation is too wide and they are not interesting to compare with experiment.

lational symmetry breaking induced by the presence of disorder, as confirmed by the increase in the transitions related MME magnitude for increasing clustering degree [36]. Such an effect causes an increment of the radiative coefficient value when the nonuniformity of the structure increases. We could interpret the increase of the global B as the onset of the transition from QW to quantum dot like behavior, induced by the high degree of clustering, as suggested by the wave functions localization depicted in Fig. 6.

Finally, in order to obtain the temperature behavior of the radiative coefficient, we derived the occupation of the states using several values of temperature and adjusting the quasi Fermi levels so that the mean carrier density is fixed. The temperature dependence of the global B so obtained is shown in Fig. 8 for several values of the mean carrier density. Only for the 100% uniform structure, the radiative coefficient $\bar{B}$ decreases with increasing temperature for all the considered values of the mean carrier density. This is compatible with simple QW theory, which predicts B to be proportional to the inverse of the temperature[40]. For increasing nonuniformity, the temperature dependence of $\bar{B}$ becomes mostly constant or even increasing with temperature, in net contrast with theory. In fact, when nonuniformities are considered, strongly localized states are present that are located deeply inside the energy gap of the 100% uniform samples, as we discussed in Sec. III A. The MME related to the low energy optical transitions between localized states of nonuniform structures have lower values with respect to the MME associated to higher energy transitions, as shown in Figure 1 of Supplemental Material [36]. Thus, at low temperature, as the occupied states are mostly localized states, the radiative coefficient is lower with respect to the B value derived for higher temperatures, when the occupation of delocalized states becomes more important. Interestingly, this behaviour better matches the measured data presented by Nippert et al.[19] for a blue multi quantum well LED, presumably having slightly lower indium content, and reported in the figure by black circles. In particular, the experimental trend is very similar to the behavior predicted for the 60% uniform structure with $\bar{n} = 5 \times 10^{11}$ cm^{-2}. Note that we are considering the temperature dependence of B and not its magnitude, that clearly differs from experiment since the simulated device has not exactly the same structural parameters as those of the LED analyzed by Nippert et al.[19], so that in particular QCSE could be different.

IV. CONCLUSIONS

In conclusion, we considered the effect of small to moderate deviations from a random alloy structure on the optical properties of bulk $In_{0.2}Ga_{0.8}N$ and InGaN/GaN SQW LED. We found that, accounting for the nonuniformity of the alloy composition, band tails appear in the calculated DOS, inducing a reduction of the band gap energy and a broadening of the optical absorption edge, in agreement with the experimental results. In turn, the decrease of the band gap yields a lower peak emission energy of the LED device, as the clustering degree increases. Furthermore, the indium content fluctuations determine a substantial broadening of the LED's optical emission spectrum. As a matter of fact, both the experimental peak energy and width are better described

when alloy nonuniformity is taken into account. Nevertheless, with our work we do not intend to rule out other mechanisms, such as excitonic effects, interface roughness [22, 42, 43], built-in field and local field effects [16, 44], which also lead to broadening and peak emission reduction. Finally, when the presence of nonuniformity is considered, a higher number of optical transitions is allowed due to the translational symmetry breaking induced by clusters. This causes the radiative coefficient to increase for increasing amount of clustering, suggesting a transition to a quantum dot like structure. We found that the experimental temperature dependence of the radiative coefficient can be well reproduced when assuming a nonuniform alloy. This is an interesting result, since the temperature behavior of B derived by standard theoretical considerations is opposite to the experimental trend.

V. ACKNOWLEDGMENTS

This work has been supported by Horizon 2020 project ChipScope, under grant agreement number 737089.

[1] S. Nakamura, M. Senoh, and T. Mukai, P-GaN/n-InGaN/n-GaN double-heterostructure blue-light-emitting diodes, Japanese Journal of Applied Physics **32**, L8 (1993).

[2] S. Nakamura, Present performance of InGaN-based blue/green/yellow LEDs, in *Light-Emitting Diodes: Research, Manufacturing, and Applications*, Vol. 3002 (International Society for Optics and Photonics, 1997) pp. 26–36.

[3] H.-M. Kim, Y.-H. Cho, H. Lee, S. I. Kim, S. R. Ryu, D. Y. Kim, T. W. Kang, and K. S. Chung, High-Brightness Light Emitting Diodes Using Dislocation-Free Indium Gallium Nitride/Gallium Nitride Multiquantum-Well Nanorod Arrays, Nano Letters **4**, 1059 (2004).

[4] H. S. El-Ghoroury, M. Yeh, J. C. Chen, X. Li, and C.-L. Chuang, Growth of monolithic full-color GaN-based LED with intermediate carrier blocking layers, AIP Advances **6**, 075316 (2016).

[5] E. Taylor, P. R. Edwards, and R. W. Martin, Colorimetry and efficiency of white LEDs: Spectral width dependence, physica status solidi (a) **209**, 461 (2012).

[6] J. Piprek, Efficiency droop in nitride-based light-emitting diodes, physica status solidi (a) **207**, 2217 (2010).

[7] M. Auf der Maur, A. Pecchia, G. Penazzi, W. Rodrigues, and A. Di Carlo, Efficiency drop in green InGaN/GaN light emitting diodes: The role of random alloy fluctuations, Phys. Rev. Lett. **116**, 027401 (2016).

[8] C. M. Jones, C.-H. Teng, Q. Yan, P.-C. Ku, and E. Kioupakis, Impact of carrier localization on recombination in InGaN quantum wells and the efficiency of nitride light-emitting diodes: Insights from theory and numerical simulations, Applied Physics Letters **111**, 113501 (2017).

[9] M. J. Galtrey, R. A. Oliver, M. J. Kappers, C. J. Humphreys, D. J. Stokes, P. H. Clifton, and A. Cerezo, Three-dimensional atom probe studies of an $In_xGa_{1-x}N$/GaN multiple quantum well structure: Assessment of possible indium clustering, Applied Physics Letters **90**, 061903 (2007).

[10] M. J. Galtrey, R. A. Oliver, M. J. Kappers, C. J. Humphreys, P. H. Clifton, A. Cerezo, and G. D. W. Smith, Response to Comment on Three-dimensional atom probe studies of an $In_xGa_{1-x}N$/GaN multiple quantum well structure: assessment of possible indium clustering, Applied Physics Letters **91**, 176102 (2007).

[11] J. A. Chan, J. Z. Liu, and A. Zunger, Bridging the gap between atomic microstructure and electronic properties of alloys: The case of (In,Ga)N, Phys. Rev. B **82**, 045112 (2010).

[12] K. H. Baloch, A. C. Johnston-Peck, K. Kisslinger, E. A. Stach, and S. Gradeak, Revisiting the In-clustering question in InGaN through the use of aberration-corrected electron microscopy below the knock-on threshold, Applied Physics Letters **102**, 191910 (2013).

[13] T.-J. Yang, R. Shivaraman, J. S. Speck, and Y.-R. Wu, The influence of random indium alloy fluctuations in indium gallium nitride quantum wells on the device behavior, Journal of Applied Physics **116**, 113104 (2014).

[14] M. Lpez, A. Pecchia, M. Auf der Maur, F. Sacconi, G. Penazzi, and A. Di Carlo, Atomistic simulations of InGaN/GaN random alloy quantum well LEDs, physica status solidi c **11**, 632 (2014).

[15] P. R. C. Kent and A. Zunger, Carrier localization and the origin of luminescence in cubic InGaN alloys, Applied Physics Letters **79**, 1977 (2001).

[16] M. A. Caro, S. Schulz, and E. P. O'Reilly, Theory of local electric polarization and its relation to internal strain: Impact on polarization potential and electronic properties of group-III nitrides, Phys. Rev. B **88**, 214103 (2013).

[17] Z. Li, J. Kang, B. Wei Wang, H. Li, Y. Hsiang Weng, Y.-C. Lee, Z. Liu, X. Yi, Z. Chuan Feng, and G. Wang, Two distinct carrier localization in green light-emitting diodes with InGaN/GaN multiple quantum wells, Journal of Applied Physics **115**, 083112 (2014).

[18] S. Schulz, M. A. Caro, C. Coughlan, and E. P. O'Reilly, Atomistic analysis of the impact of alloy and well-width fluctuations on the electronic and optical properties of InGaN/GaN quantum wells, Phys. Rev. B **91**, 035439 (2015).

[19] F. Nippert, S. Y. Karpov, G. Callsen, B. Galler, T. Kure, C. Nenstiel, M. R. Wagner, M. Straburg, H.-J. Lugauer, and A. Hoffmann, Temperature-dependent recombination coefficients in InGaN light-emitting diodes: Hole localization, Auger processes, and the green gap, Applied Physics Letters **109**, 161103 (2016).

[20] B. Lee and L. W. Wang, Band gap bowing and electron localization of $Ga_xIn_{1-x}N$, Journal of Applied Physics **100**, 093717 (2006).

[21] D. Oriato and A. B. Walker, Effects of piezoelectric field, bias and indium fluctuations on a InGaNGaN single quantum well system, Physica B: Condensed Mat-

ter **314**, 59 (2002), proceedings of the Twelfth International Conference on Nonequilib rium Carrier Dynamics in Semiconductors.

[22] D. S. P. Tanner, J. M. McMahon, and S. Schulz, Interface Roughness, Carrier Localization, and Wave Function Overlap in c-Plane $(In, Ga)N/GaN$ Quantum Wells: Interplay of Well Width, Alloy Microstructure, Structural Inhomogeneities, and Coulomb Effects, Phys. Rev. Applied **10**, 034027 (2018).

[23] X. Wu, E. J. Walter, A. M. Rappe, R. Car, and A. Selloni, Hybrid density functional calculations of the band gap of $Ga_xIn_{1-x}N$, Phys. Rev. B **80**, 115201 (2009).

[24] I. Gorczyca, S. P. Łepkowski, T. Suski, N. E. Christensen, and A. Svane, Influence of indium clustering on the band structure of semiconducting ternary and quaternary nitride alloys, Phys. Rev. B **80**, 075202 (2009).

[25] J.-M. Jancu, R. Scholz, F. Beltram, and F. Bassani, Empirical $spds^*$ tight-binding calculation for cubic semiconductors: General method and material parameters, Phys. Rev. B **57**, 6493 (1998).

[26] J.-M. Jancu, F. Bassani, F. D. Sala, and R. Scholz, Transferable tight-binding parametrization for the group-III nitrides, Applied Physics Letters **81**, 4838 (2002).

[27] D. Camacho and Y. Niquet, Application of Keating's valence force field model to non-ideal wurtzite materials, Physica E: Low-dimensional Systems and Nanostructures **42**, 1361 (2010).

[28] D. Watson-Parris, M. J. Godfrey, P. Dawson, R. A. Oliver, M. J. Galtrey, M. J. Kappers, and C. J. Humphreys, Carrier localization mechanisms in $In_xGa_{1-x}N/GaN$ quantum wells, Phys. Rev. B **83**, 115321 (2011).

[29] TiberCAD simulation package, `http://www.tibercad.org`.

[30] L. Bellaiche, T. Mattila, L.-W. Wang, S.-H. Wei, and A. Zunger, Resonant hole localization and anomalous optical bowing in InGaN alloys, Applied Physics Letters **74**, 1842 (1999).

[31] I. Gorczyca, T. Suski, N. E. Christensen, and A. Svane, Gap bowing in $In_xGa_{1x}N$ and $In_xAl_{1x}N$ under pressure, physica status solidi c **6**, S368 (2009).

[32] K. A. Mder and A. Zunger, Effects of atomic clustering on the optical properties of IIIV alloys, Applied Physics Letters **64**, 2882 (1994).

[33] J. Wu, W. Walukiewicz, K. M. Yu, J. W. Ager, E. E. Haller, H. Lu, and W. J. Schaff, Small band gap bowing in $In_{1x}Ga_xN$ alloys, Applied Physics Letters **80**, 4741 (2002).

[34] G. Franssen, I. Gorczyca, T. Suski, A. Kamiska, J. Pereiro, E. Muoz, E. Iliopoulos, A. Georgakilas, S. B. Che, Y. Ishitani, A. Yoshikawa, N. E. Christensen, and A. Svane, Bowing of the band gap pressure coefficient in $In_xGa_{1x}N$ alloys, Journal of Applied Physics **103**, 033514 (2008).

[35] M. Moret, B. Gil, S. Ruffenach, O. Briot, C. Giesen, M. Heuken, S. Rushworth, T. Leese, and M. Succi, Optical, structural investigations and band-gap bowing parameter of GaInN alloys, Journal of Crystal Growth **311**, 2795 (2009), proceedings of the "2nd International Symposium on Growth of III Nitrides.

[36] See Supplemental Material at, URL, for the analysis of the indium distribution within the samples and the description of the clustering induced carrier localization and translational symmetry breaking.

[37] R. Butté, L. Lahourcade, T. K. Udavinys, G. Callsen, M. Mensi, M. Glauser, G. Rossbach, D. Martin, J.-F. Carlin, S. Marcinkeviius, and N. Grandjean, Optical absorption edge broadening in thick InGaN layers: Random alloy atomic disorder and growth mode induced fluctuations, Applied Physics Letters **112**, 032106 (2018).

[38] M. Auf der Maur, B. Galler, I. Pietzonka, M. Strassburg, H. Lugauer, and A. Di Carlo, Trap-assisted tunneling in InGaN/GaN single-quantum-well light-emitting diodes, Applied Physics Letters **105**, 133504 (2014).

[39] L. Rigutti, L. Mancini, D. Hernndez-Maldonado, W. Lefebvre, E. Giraud, R. Butt, J. F. Carlin, N. Grandjean, D. Blavette, and F. Vurpillot, Statistical correction of atom probe tomography data of semiconductor alloys combined with optical spectroscopy: The case of $Al_{0.25}Ga_{0.75}N$, Journal of Applied Physics **119**, 105704 (2016).

[40] P. K. Basu, *Theory of optical processes in semiconductors: bulk and microstructures*, Vol. 4 (Clarendon press, 1997).

[41] As confirmed by personal communication of the author.

[42] M. J. Galtrey, R. A. Oliver, M. J. Kappers, C. J. Humphreys, P. H. Clifton, D. Larson, D. W. Saxey, and A. Cerezo, Three-dimensional atom probe analysis of green- and blue-emitting In_xGa_{1x}NGaN multiple quantum well structures, Journal of Applied Physics **104**, 013524 (2008).

[43] C.-K. Tan, W. Sun, J. J. Wierer Jr, and N. Tansu, Effect of interface roughness on auger recombination in semiconductor quantum wells, AIP Advances **7**, 035212 (2017).

[44] M. Baranowski, Ł. Janicki, M. Gladysiewicz, M. Wełna, M. Latkowska, J. Misiewicz, Ł. Marona, D. Schiavon, P. Perlin, and R. Kudrawiec, Direct evidence of photoluminescence broadening enhancement by local electric field fluctuations in polar InGaN/GaN quantum wells, Japanese Journal of Applied Physics **57**, 020305 (2018).